A New Wideband Adaptive Digital Predistortion Technique Employing Feedback Linearization

Jangheon Kim, *Student Member, IEEE*, Young Yun Woo, Junghwan Moon, and Bumman Kim, *Fellow, IEEE*

***Abstract*—We develop a new wideband digital feedback predistortion (WDFBPD) technique for modulated signals with wide bandwidths by combining digital feedback predistortion (DFBPD) linearization and memory-effect compensation techniques. For the experiments, a class-AB amplifier using an LDMOSFET with 90-W peak envelope power is employed. The proposed technique is compared with existing DFBPD and memory polynomial (MP) techniques for a 2.14-GHz forward-link WCDMA 2FA signal with 10-MHz carrier spacing. The experimental results show that the new WDFBPD technique has better linearization performance than conventional DFBPD and lower computational complexity than the MP technique.**

***Index Terms*—Memory effects, power amplifier (PA), predistortion (PD), wideband code division multiple access (WCDMA).**

I. Introduction

CURRENT wireless communication systems have progressed to transmit high data-rate signals for multimedia communications in a fast moving environment. The modulated signals of these systems vary rapidly and have high peak-to-average power ratios (PAPRs). In order to linearly amplify the signals, digital predistortion (DPD) techniques have been widely used and studied [1]–[6].

For various communication signals with wide bandwidths, such as multicarrier wideband code division multiple access (WCDMA), wireless local area network (WLAN), worldwide interoperability for microwave access (WiMAX), etc., the memory-effect compensation is an important issue of the DPD algorithm in addition to correction of power amplifier (PA) nonlinearity. The memory effects are defined as changes of the amplitude and phase in distortion components due to past signal values. To characterize these effects, two-tone signals with varying tone spacings are applied to the amplifier, which causes asymmetrical and tone-spacing-dependent intermodulation distortion (IMD). Moreover, the memory effects generate unbalanced spurious emissions for modulated signals [7]–[11]. For this bandwidth-dependent distortion, memoryless DPD techniques cannot properly cancel the distortion. Therefore, the predistortion (PD) algorithm has to include a memory compensation mechanism, and such algorithms have been extensively studied [12]–[18].

Recently, new DPD techniques based on feedback concepts have been introduced, and these techniques avoid the bandwidth limitation of feedback systems by employing the lookup table (LUT) concept for feedback signal estimation in the digital domain. Chung *et al.* [19] have presented an open-loop DPD technique using a Cartesian LUT and analog Cartesian feedback based on feedback linearization. This technique realizes a minimum of power overhead associated with linearization, a minimum of PA modeling, and no model convergence issue for portable communication units. In our group, the digital feedback predistortion (DFBPD) technique for base-station transmitters, based on feedback PD [20], has been developed [21]. The DFBPD technique has advantages such as a simple PD algorithm, fast convergence speed, accurate PD signal extraction, and better system tolerance. Due to these advantages, this technique can successfully linearize nonstandard nonlinear characteristics of Doherty and saturated amplifiers operated at the average power level [22]. It is shown that the DFBPD technique is suitable for the linearization of highly efficient and linear PA applications. Additionally, in order to provide good linearization performance for wideband signals, a memory compensation algorithm is required for the proposed techniques because feedback only linearizes the memoryless PA nonlinearity.

In this paper, we propose a new wideband digital feedback predistortion (WDFBPD) technique by combining the inverse memory structure with the DFBPD structure. This technique not only maintains the advantages of the DFBPD technique, but also suppresses the memory effects. The predistorted signal produced by this algorithm uses the instantaneous nonlinear characteristics to compensate the memory effects, as well as the PA nonlinearity. For the experiments, a class-AB amplifier is fabricated using an LDMOSFET with 90-W peak envelope power (PEP). Before applying the PD algorithm, we have explored the nonlinear characteristics and memory effects for two-tone signals (up to 20-MHz tone spacing). From the experimental results, it will be demonstrated that the WDFBPD algorithm has better linearization performance than the DFBPD algorithm for a wideband signal and is more effective than the memory polynomial (MP) algorithm.

II. Operation of WDFBPD Technique

It is important to explore the AM/AM and AM/PM distortion of a PA in order to compensate the memory distortion effects,

Manuscript received July 25, 2007; revised October 31, 2007. This work was supported by the Korean Government under the Korea Science and Engineering Foundation (KOSEF) MOST Grant R01-2007-000-20377-0 and by the Center for Broadband Orthogonal Frequency Division Multiplex Mobile Access, Pohang University of Science and Technology under the Information Technology Research Center Program of the Korean Ministry of Information Technology, supervised by the Institute for Information Technology Advancement (IITA-2007-C1090-0701-0037).

J. Kim, J. Moon, and B. Kim are with the Department of Electrical Engineering, Pohang University of Science and Technology, Gyeongbuk 790-784, Korea (e-mail: rage3k@postech.ac.kr; jhmoon@postech.ac.kr; bmkim@postech.ac.kr).

Y. Y. Woo is with the Telecommunication Research and Development Center, Samsung Electronics Company Ltd., Suwon, Gyeonggi 442-742, Korea (e-mail: w0yun@postech.ac.kr).

Color versions of one or more of the figures in this paper are available online at http://ieeexplore.ieee.org.

Digital Object Identifier 10.1109/TMTT.2007.914362

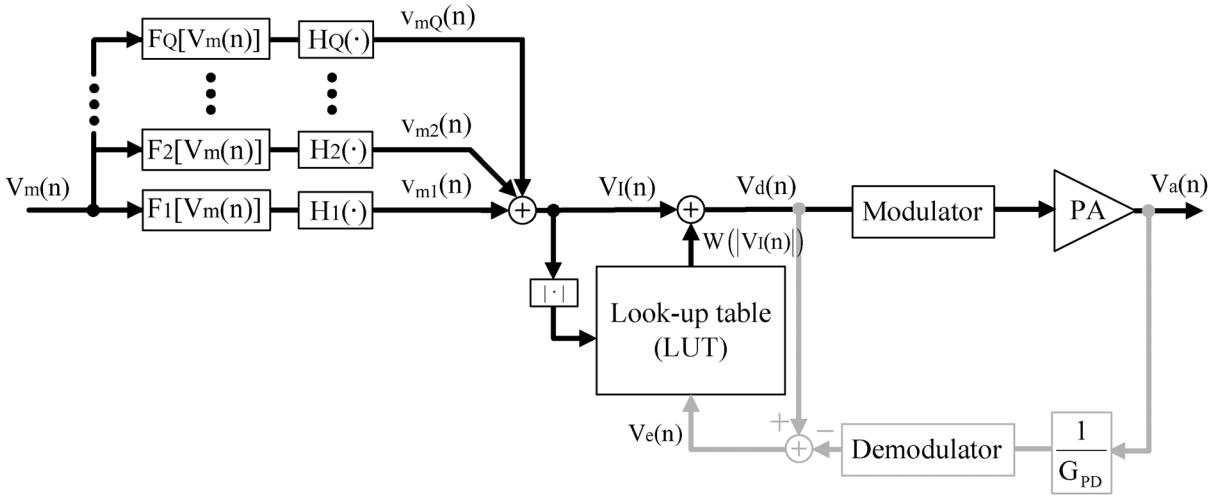

Fig. 1. Simplified block diagram of proposed wideband digital feedback predistorter.

as well as the nonlinear characteristic. PAs with memory effects generate AM/AM and AM/PM scattering around the memoryless nonlinear characteristics. The memoryless DPD algorithm can only provide limited linearization performance due to this scattering. As a result, the wideband DPD algorithm should have a memory compensation structure in addition to correction for the instantaneous nonlinear characteristic.

By combining the DFBPD and memory-effect compensation algorithms, we have developed a new WDFBPD technique, as shown in Fig. 1. The memory compensation part of the proposed technique consists of multiple branches connected in parallel. Each branch is composed of a nonlinear function $F_q(\cdot)$ and an impulse response $H_q(\cdot)$. These transform the input signal into an inverse envelope memory signal, which is combined with the instantaneous input signal, high-order input signals, and past input signals. These signals are used, in addition to the LUT error signal, as shown in Fig. 1, so that the algorithm can independently compensate for both memory effects and memoryless nonlinear characteristics. The total predistorted signal $V_{\rm d}(n)$ is expressed as

$$\begin{aligned} V_{\rm d}(n) &= W(|V_{\rm I}(n)|) + V_{\rm I}(n) \\ &= W(|V_{\rm I}(n)|) + \sum_{q=1}^{Q} V_{\rm mq}(n) \\ &= W(|V_{\rm I}(n)|) + \sum_{q=1}^{Q} H_q\{F_q[V_{\rm m}(n)]\} \\ &= W(|V_{\rm I}(n)|) + \sum_{q=1}^{Q}\sum_{l=0}^{L-1} a_{lq} F_q[V_{\rm m}(n-l)] \\ &= W(|V_{\rm I}(n)|) + \sum_{q=1}^{Q}\sum_{l=0}^{L-1} a_{lq} V_{\rm m}(n-l)|V_{\rm m}(n-l)|^{q-1} \end{aligned} \tag{1}$$

where $V_{\rm m}(n)$, $V_{\rm I}(n)$, and $W(|V_{\rm I}(n)|)$ are the modulated source, inverse scattered, and LUT output signals, respectively. Here, a_{lq} are the coefficients of the impulse response. The parameter Q specifies the number of the parallel branches and L is the memory length of the WDFBPD algorithm. In the memory compensation algorithm, because the signal caused by memory effects is composed of mixed signals for odd- and even-order components, as well as the fundamental, the nonlinear function should include those compensation polynomials. The first-order function $F_1(\cdot)$ of the impulse response is dominant, and the other components have small coefficient values. This algorithm can linearize memory effects using a simplified MP structure because the nonlinearity is completely compensated by the DFBPD algorithm.

Fig. 2 shows a flow diagram of the WDFBPD algorithm. In the first part, the PA is modeled from its input and output measurements using the weighted polynomial modeling method [23]. In the next part, the predistorted signal, which compensates the memoryless PA nonlinearity, is constructed using the DFBPD algorithm with the condition of $Q = 1$ and $L = 0 (V_{\rm m} = V_{\rm I})$, and the linearization of the amplifier is performed through several iterations [21]. In this process, the data in the LUT can be constructed as a function of the input for the training sequence with time samples, $n = 1, 2, \ldots, N$, at low speed. This algorithm can be written as follows:

$$\begin{aligned} W^k(|V_{\rm I}(n)|) &= V_{\rm e}^{k-1}(n)|_{|V_{\rm I}(n)|} \\ &= \left[V_{\rm d}^{k-1}(n) - \frac{V_{\rm a}^{k-1}(n)}{G_{\rm PD}}\right]\Bigg|_{|V_{\rm I}(n)|} \end{aligned} \tag{2}$$

for iteration

$$k = 1, 2, \ldots, K \tag{3}$$

where $V_{\rm e}^{k-1}(n)$ is the error signal and $G_{\rm PD}$ is the overall PD system gain. In real time operation, the data is supplied very fast from the constructed LUT, and the predistorted signal is generated using the data. After this procedure, the linearized amplifier input and output data ($V_{\rm m}$ and $V_{\rm a}$) are collected, and the AM/AM and AM/PM characteristics are identified from the data. To compensate the scattering characteristics caused by the

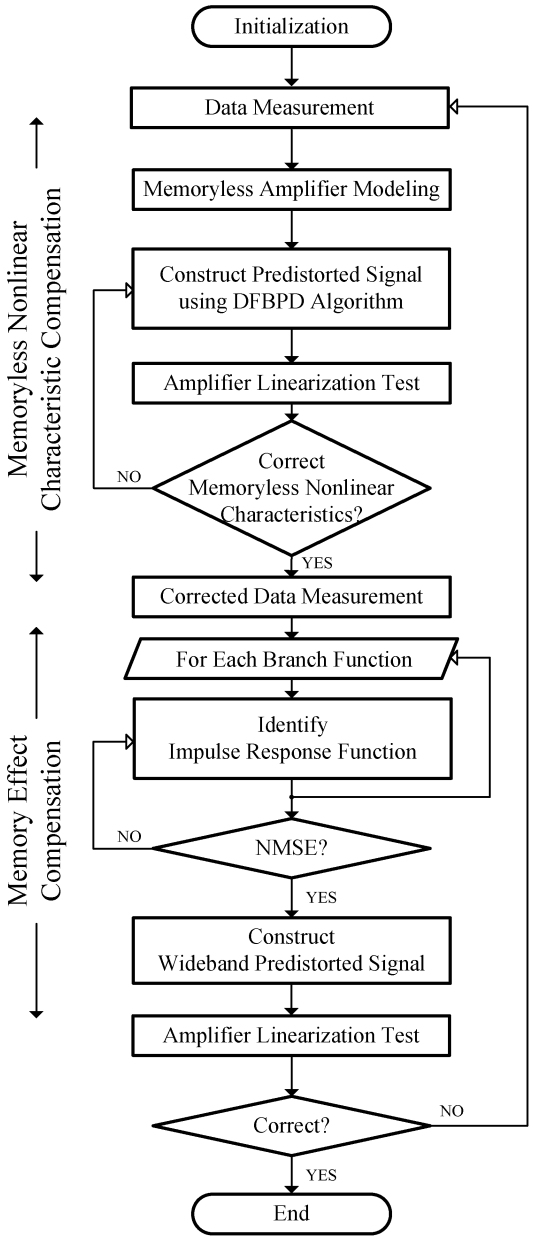

Fig. 2. Flow diagram of WDFBPD algorithm.

memory effects, the coefficients a_{lq} of the impulse response are solved using the recursive least squares (RLS) algorithm [24]. Finally, the linearization for the memoryless nonlinear characteristics and memory effects are accomplished simultaneously by applying the total predistorted signal of (1) to the amplifier.

To solve for the inverse scattering characteristic or the coefficients a_{lq}, the modulated source data $V_{\rm m}$ and the memoryless nonlinearity correction data $V_{\rm a}$ are used. Based on these data, we define the scattering test signal $V_{\rm t}$, which is composed of the filtered signal components attained from the nonlinear functions and impulse responses. If the data are the training sequences with time samples, $n = L, L+1, \ldots, N$, then $V_{\rm t}$ can be written in matrix format as follows:

$$V_{\rm t} = UA \tag{4}$$

where

$$V_{\rm t} = [V_{\rm t}(L)V_{\rm t}(L+1)\cdots V_{\rm t}(n)\cdots V_{\rm t}(N)]^T$$
$$A = [A_1 A_2 \cdots A_Q]^T$$
$$A_q = [a_{0q}a_{1q}\cdots a_{(L-1)q}]^T$$
$$U = \begin{bmatrix} U_1(L) & U_2(L) & \cdots & U_Q(L) \\ U_1(L+1) & U_2(L+1) & \cdots & U_Q(L+1) \\ \vdots & \vdots & \ddots & \vdots \\ U_1(n) & U_2(n) & \cdots & U_Q(n) \\ \vdots & \vdots & \ddots & \vdots \\ U_1(N) & U_2(N) & \cdots & U_Q(N) \end{bmatrix}$$
$$U_q(n) = \begin{bmatrix} V_{\rm a}(n-0)|V_{\rm a}(n-0)|^{q-1} \\ V_{\rm a}(n-1)|V_{\rm a}(n-1)|^{q-1} \\ \vdots \\ V_{\rm a}(n-L+1)|V_{\rm a}(n-L+1)|^{q-1} \end{bmatrix}^T,$$
$$q = 1, 2, \ldots, Q.$$

The RLS algorithm process to solve for the coefficients is given as follows: $A_q(0)$ and $P(0)$ are initialized as

$$A_q(0) = [0\,0\,0\cdots 0\,0]^T \tag{5}$$
$$P(0) = \delta^{-1} I \tag{6}$$

where δ is a small positive constant, $A_q(0)$ is a $L \times 1$ vector, and I is the $LQ \times LQ$ identity matrix. Next, the RLS algorithm is computed for time samples n as

$$\pi(n) = P(n-1)V_{\rm t}(n) \tag{7}$$
$$K(n) = \frac{\pi(n)}{\lambda + V_{\rm t}^H(n)\pi(n)} \tag{8}$$
$$e(n) = V_{\rm m}(n) - \frac{V_{\rm t}(n)}{G_L} \tag{9}$$
$$A(n) = A(n-1) + K(n)e^*(n) \tag{10}$$
$$P(n) = \lambda^{-1}P(n-1) - \lambda^{-1}K(n)V_{\rm t}^H(n)P(n-1) \tag{11}$$

where λ is the forgetting factor (a scalar value), G_L is the linear gain between $V_{\rm m}$ and $V_{\rm a}$, and $P(n)$ is an $LQ \times LQ$ matrix. Both $\pi(n)$ and $K(n)$ are $LQ \times 1$ vectors. Thus, the estimation error $e(n)$ is minimized by each successive iteration so that the coefficients a_{lq} of the impulse response are constructed and also updated. An important feature of the RLS algorithm is that the inversion of the correlation matrix is replaced at each step by a simple scalar division.

III. Implementation and Measurement Results

A. Two-Tone Test

We have built a PA using the Freescale MRF5S21090 LDMOSFET with 90-W PEP in class-AB operation at $I_{\rm DS} = 0.75$ A and $V_{\rm DD} = 27$ V, and have optimized the linearity and efficiency to be as high as possible. Before applying the PD algorithm, we have explored the nonlinear characteristics and memory effects using two-tone signals (up to 20-MHz tone spacing). Fig. 3 illustrates the third-order intermodulation distortion (IMD3) and fifth-order intermodulation distortion (IMD5) for the two-tone signals. This amplifier has

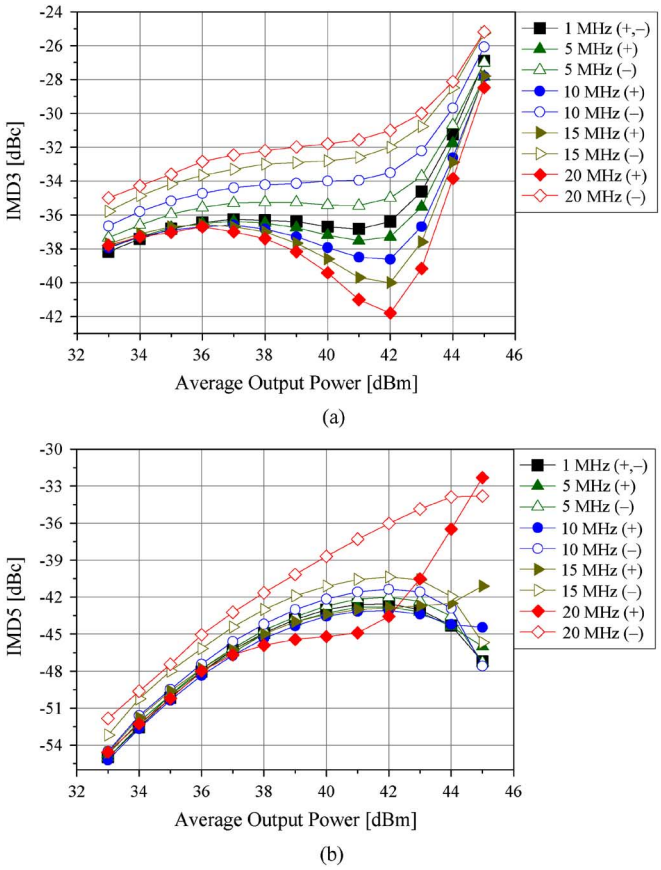

Fig. 3. Measured: (a) IMD3 and (b) IMD5 characteristics for two-tone signals.

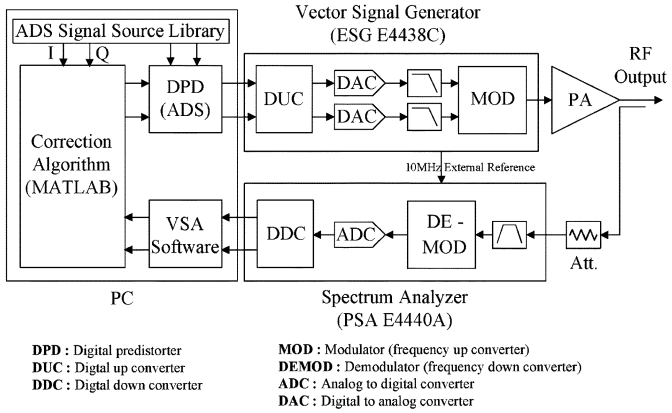

Fig. 4. Experimental setup for linearization test.

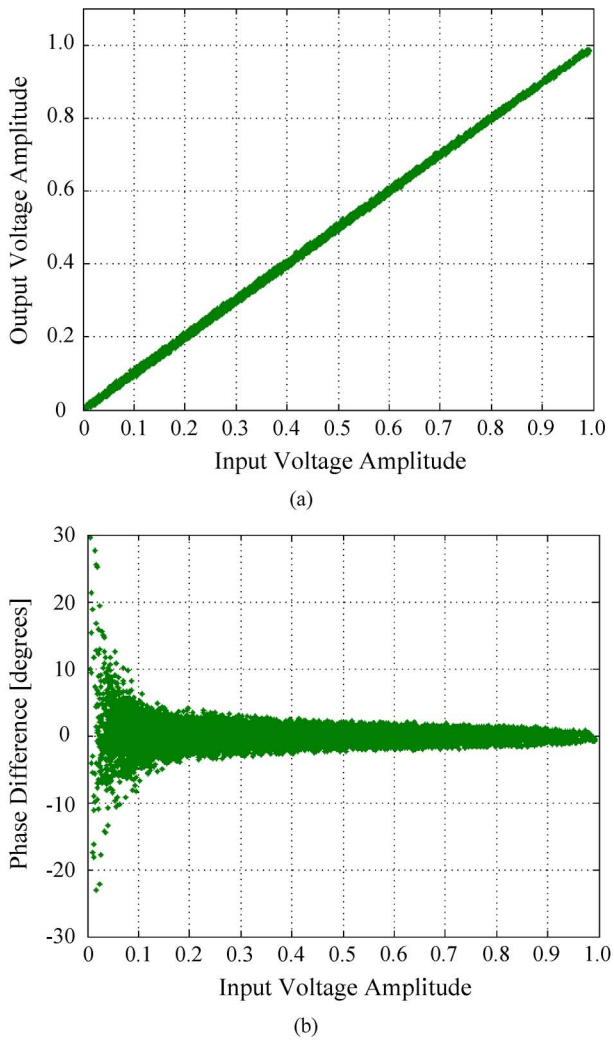

Fig. 5. Measured: (a) AM/AM and (b) AM/PM characteristics after DFBPD linearization at an average output power of 40 dBm for the WCDMA 2FA signal with 10-MHz carrier spacing.

relatively serious high-order memory effects, as can be seen from the differences between the upper and lower sidebands of IMD3 and IMD5 (approximately 6-dB difference at average output powers from 40 to 43 dBm). The IMD3s and IMD5s are not monotonic over the entire output power range. Also, the upper IMD3s increase while the lower IMD3s decrease due to the memory effects. This IMD3 difference has a maximum value of 11 dB at an average output power of 42 dBm. Moreover, the IMD5s represent moderate characteristics up to 15-MHz tone spacing, but change abruptly for 20-MHz tone spacing. The amplifier generates higher spurious emission in the lower band than in the upper band for a wideband signal. Therefore, the digital predistorter should generate a higher predistorted signal in the lower frequency band than in the upper frequency band.

B. WCDMA 2FA Test With 10-MHz Carrier Spacing

To validate the proposed algorithm for the linearization of wideband signals, we have employed a 2.14-GHz forward-link WCDMA 2FA signal with 10-MHz carrier spacing (15-MHz bandwidth) and 7.4-dB PAPR at the 0.01% level of the complementary cumulative distribution function (CCDF). The Agilent Advanced Design System (ADS) using an electronic signal generator (ESG) and vector signal analyzer (VSA) connected solution was used for the test, as shown in Fig. 4 [25]. The proposed algorithm has two 256-entry AM/AM and AM/PM LUTs and the memory compensation on the left side of Fig. 1, which are programmed by MATLAB using the DFBPD and RLS algorithms, respectively. The linearization capability of the proposed algorithm is evaluated using the implemented amplifier with serious memory effects and compared with the DFBPD and MP algorithms.

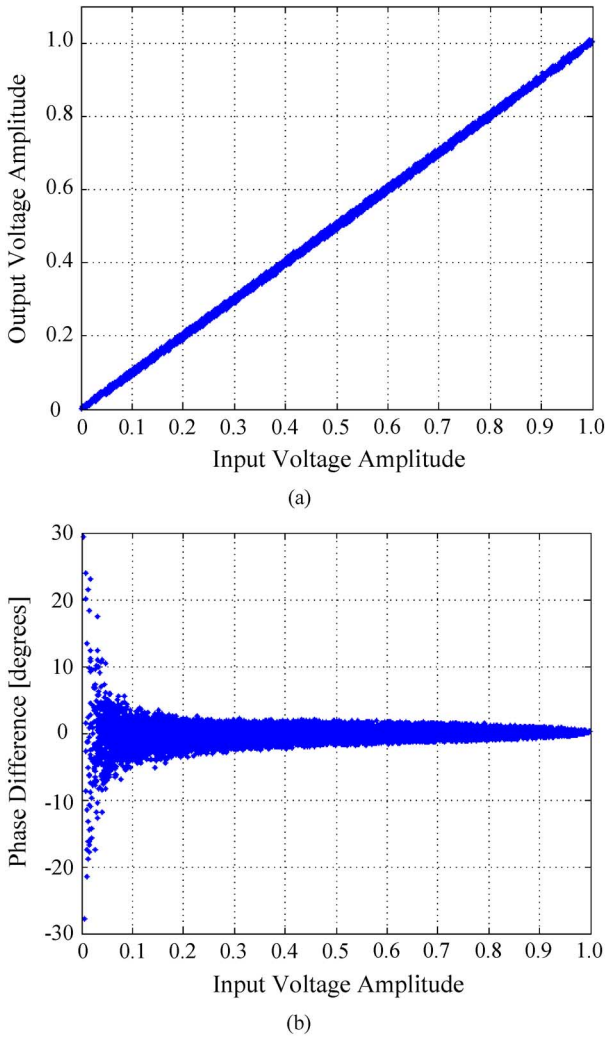

Fig. 6. Measured: (a) AM/AM and (b) AM/PM characteristics of the inverse scattering signal V_{I} predistorted to compensate the memory effects for the WCDMA 2FA signal with 10-MHz carrier spacing.

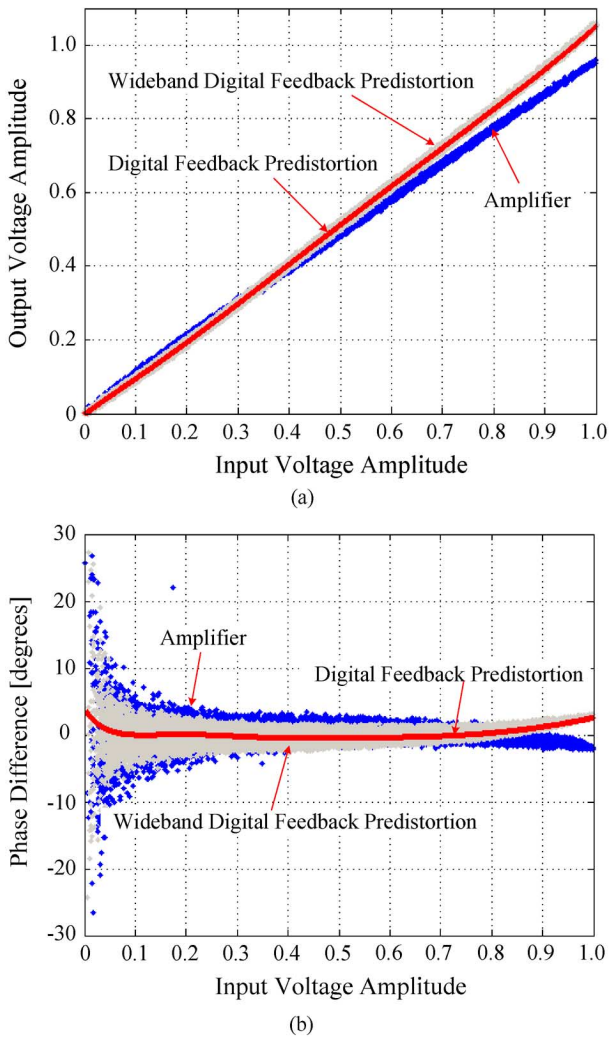

Fig. 7. Measured predistorted: (a) AM/AM and (b) AM/PM characteristics before linearization and after PD by the DFBPD and WDFBPD algorithms for the WCDMA 2FA signal with 10-MHz carrier spacing.

Fig. 5 shows the AM/AM and AM/PM characteristics of the amplifier after linearization by the DFBPD algorithm. The memoryless nonlinear characteristics are linearized, but the algorithm cannot reduce the scattering of the output signals caused by memory effects. To compensate the scattering, the memory compensation algorithm of the WDFBPD technique with a second-order nonlinear function $(Q = 2)$ and five memory taps $(L = 5)$ is required, and the coefficients a_{lq} are solved for using the RLS algorithm. Fig. 6 shows the AM/AM and AM/PM characteristics of the inverse scattered input $V_{\mathrm{I}}(n)$, which is predistorted to compensate the memory effects only, and represents the inverse scattering characteristics of the amplifier output shown in Fig. 5.

Fig. 7 shows the AM/AM and AM/PM characteristics before linearization and after PD by the DFBPD and WDFBPD algorithms. The DFBPD algorithm provides the memoryless predistorted signal to compensate the memoryless nonlinear characteristics, while the WDFBPD algorithm generates the memory predistorted signal to linearize the bandwidth-dependent nonlinear characteristics. The predistorted signal produced by the WDFBPD algorithm assures that the memory compensation is properly combined with the DFBPD linearization algorithm. Fig. 8 shows the measured spectra of the predistorted signals generated by the DFBPD and WDFBPD algorithms. As mentioned in Section III-A, the amplifier exhibits higher spurious emission in the lower frequency band than in the upper frequency band. As shown in Fig. 8, the DFBPD algorithm provides balanced spurious emission, but the WDFBPD algorithm generates unbalanced spurious emission, reflecting the memory effects.

Fig. 9 shows the measured AM/AM and AM/PM characteristics at the amplifier output after DFBPD and WDFBPD linearization at an average output power of 40 dBm for the WCDMA 2FA signal with 10-MHz carrier spacing. The nonlinear characteristics are successfully linearized by both linearization algorithms. However, the AM/AM and AM/PM scattering is better suppressed by the WDFBPD linearization due to the memory-effect compensation. Fig. 10 shows the measured WCDMA 2FA spectra before and after DFBPD and WDFBPD linearization at an average output power of 40 dBm. The adjacent channel leakage ratio (ACLR) at an offset of 10 MHz for the WDFBPD algorithm is −57.3 dBc, which is an improvement of

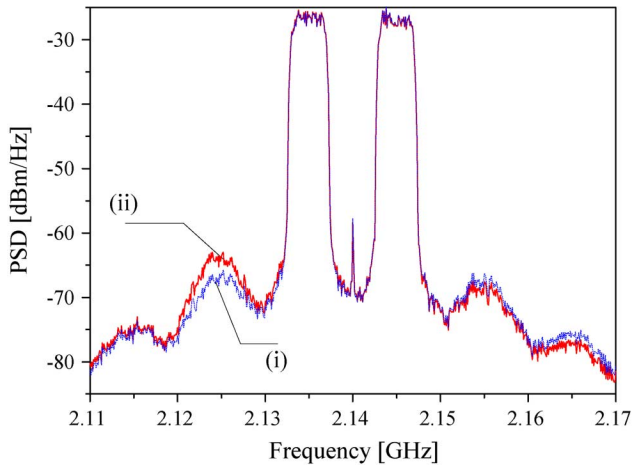

Fig. 8. Measured WCDMA 2FA spectra of predistorted signals. (i) Digital feedback predistorter. (ii) Wideband digital feedback predistorter.

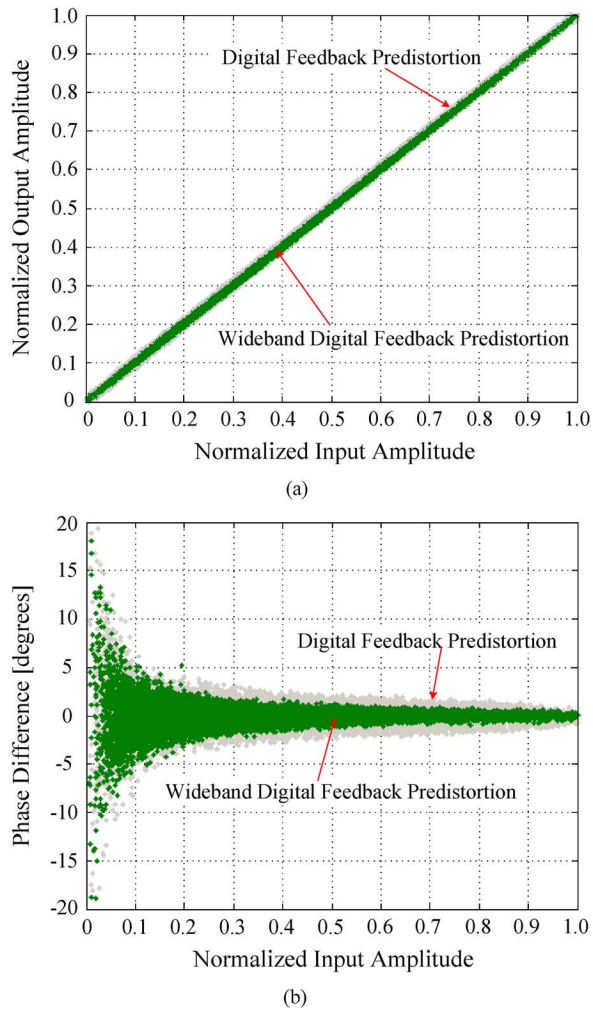

Fig. 9. Measured: (a) AM/AM and (b) AM/PM output characteristics after DFBPD and WDFBPD linearization at an average output power of 40 dBm for the WCDMA 2FA signal with 10-MHz carrier spacing.

approximately 17.7 dB at the same average output power. Additionally, the error vector magnitude (EVM) is 0.95%, an improvement of approximately 2.65% at the same output power.

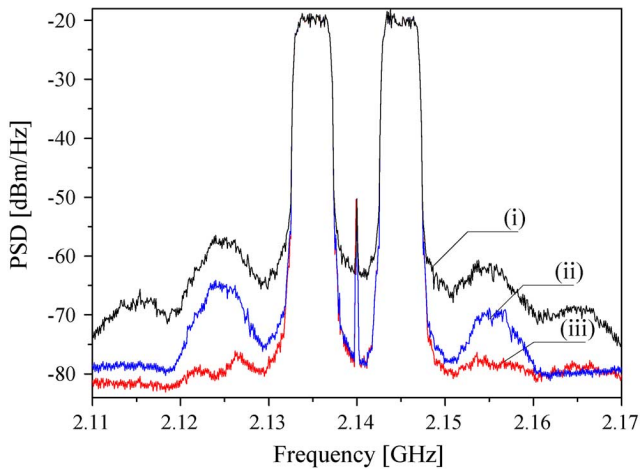

Fig. 10. Measured WCDMA 2FA spectra before and after linearization. (i) Without predistorter. (ii) Digital feedback predistorter. (iii) Wideband digital feedback predistorter.

TABLE I
MEASURED PERFORMANCE BEFORE AND AFTER LINEARIZATION AT AN AVERAGE OUTPUT POWER OF 40 dBm FOR WCDMA 2FA SIGNAL WITH 10-MHz CARRIER SPACING

	ACLR [dBc] at –/ +10-MHz	EVM [%]
Amplifier	–39.6/ –42.0	3.60
DFBPD + Amp.	–45.1/ –49.6	1.70
WDFBPD + Amp.	–57.9/ –57.3	0.95

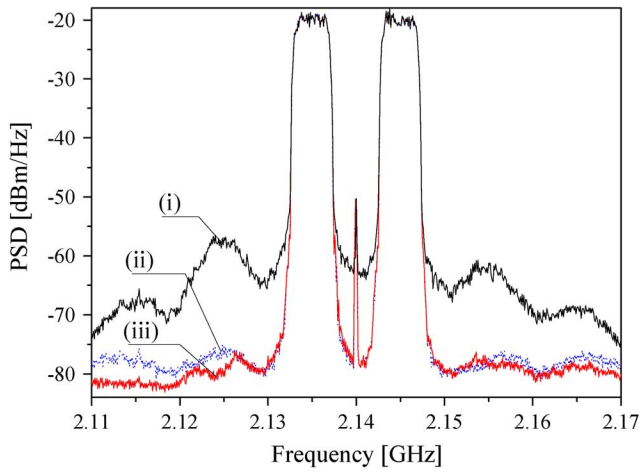

Fig. 11. Measured WCDMA 2FA spectra before and after linearization. (i) Without predistorter. (ii) MP predistorter. (iii) Wideband digital feedback predistorter.

In comparison with the DFBPD algorithm, the WDFBPD algorithm delivers improved linearization due to the memory-effect compensation. The measurement results are summarized in Table I.

Fig. 11 shows the measured WCDMA 2FA spectra after MP [13], [17] and WDFBPD linearizations at the same output power. The predistorted signal of the MP is expressed as

$$V_{\mathrm{d,MP}}(n) = \sum_{k=1}^{K} \sum_{j=0}^{J-1} a_{jk} V_{\mathrm{m}}(n-j) |V_{\mathrm{m}} \times (n-j)|^{k-1}. \quad (12)$$

TABLE II
MEASURED PERFORMANCE AFTER MP AND WDFBPD LINEARIZATION AT AN AVERAGE OUTPUT POWER OF 40 dBm FOR WCDMA 2FA SIGNAL WITH 10-MHz CARRIER SPACING

Linearization Technique	Predistorted Signal	Polynomial Order	Memory Length	# of Coeffs.	ACLR [dBc] at $-/+10$-MHz	EVM [%]
MP	$V_{\mathrm{d,MP}}(n)=\sum_{k=1}^{K}\sum_{j=0}^{J-1}a_{jk}V_{\mathrm{m}}(n-j)\lvert V_{\mathrm{m}}(n-j)\rvert^{k-1}$	$K=7$	$J=5$	35	$-54.5/-57.3$	1.03
WDFBPD	$V_{\mathrm{d,WDFBPD}}(n)=W(n)+\sum_{q=1}^{Q}\sum_{l=0}^{L-1}a_{lq}V_{\mathrm{m}}(n-l)\lvert V_{\mathrm{m}}(n-l)\rvert^{q-1}$	$Q=2$	$L=5$	10	$-57.9/-57.3$	0.95

The MP algorithm is set to a seventh-order polynomial ($K=7$) and five delay taps ($J=5$), which represent a total 35 coefficients, and the coefficients a_{jk} are solved for using the RLS algorithm. The ACLR at an offset of 10 MHz and EVM are -54.5 dBc and 1.03%, respectively. In comparison with the WDFBPD algorithm, the MP algorithm delivers similar linearization performance, but requires more coefficients to compensate the nonlinear characteristics and memory effects. Since it requires the inversion of a Vandermonde matrix of size $(N-L+1)\times JK$ to solve these coefficients, the MP has higher computational complexity than that of the WDFBPD algorithm, which requires the inversion of a Vandermonde matrix of size $(N-L+1)\times LQ$ and the very simple DFBPD algorithm. This fact assures that the proposed algorithm can reduce the field programmable gate array (FPGA) resource or digital signal processing (DSP) computational load in terms of the algorithm implementation.

The experimental results show that the WDFBPD algorithm can successfully linearize memory effects using a simplified MP structure because the nonlinearity is efficiently compensated by the DFBPD algorithm and the inverse memory signal is mainly generated by the fundamental component and a few harmonics. The measurement results and linearization conditions are summarized in Table II.

IV. CONCLUSION

We have proposed a new PD algorithm based on the feedback PD technique combined with the MP structure. The algorithm provides highly efficient nonlinearity compensation by the DFBPD method, and the MP becomes very simplified, requiring only a second-order nonlinearity and five memory taps. For the experiments, a class-AB amplifier is fabricated using an LDMOSFET with a 90-W PEP. We have explored the nonlinear characteristics and memory effects for two-tone signals (up to 20-MHz tone spacing). From the two-tone test, the implemented amplifier exhibits serious memory effects. For a 2.14-GHz forward-link WCDMA 2FA signal with 10-MHz carrier spacing, the proposed WDFBPD technique provides an ACLR at 10-MHz offset and EVM of the amplifier of -57.3 dBc and 0.95%, which are improvements of 17.7 dB and 2.65%, respectively, at an average output power of 40 dBm.

From the experimental results, we conclude that the WDFBPD method can deliver better linearization performance than the DFBPD method for a wideband signal, while maintaining most of the DFBPD technique's advantages. Thus, a simpler structure is realized with the ability of faster and more accurate PD signal extraction and feedback related characteristics in comparison with conventional DPD methods. Therefore, the WDFBPD technique is a very useful linearization technique for wideband signals.

ACKNOWLEDGMENT

The authors would like to express their gratitude to the reviewers for their valuable comments and especially for editing this paper's manuscript.

REFERENCES

[1] S. C. Cripps, *RF Power Amplifiers for Wireless Communications*. Norwood, MA: Artech House, 1999.
[2] P. B. Kenington, *High-Linearity RF Amplifier Design*. Norwood, MA: Artech House, 2000.
[3] Y. Nagata, "Linear amplification techniques for digital mobile communications," in *Proc. IEEE 39th Veh. Technol. Conf.*, 1989, pp. 159–164.
[4] J. K. Cavers, "Amplifier linearization using a digital predistorter with fast adaptation and low memory requirements," *IEEE Trans. Veh. Technol.*, vol. 39, no. 4, pp. 374–382, Nov. 1990.
[5] A. S. Wright and W. G. Durtler, "Experimental performance of an adaptive digital linearized power amplifier," *IEEE Trans. Veh. Technol.*, vol. 41, no. 4, pp. 395–400, Nov. 1992.
[6] M. Faulkner and M. Johansson, "Adaptive linearization using predistortion—Experimental results," *IEEE Trans. Veh. Technol.*, vol. 43, no. 2, pp. 323–332, May 1994.
[7] J. Vuolevi and T. Rahkonen, *Distortion in RF Power Amplifiers*. Norwood, MA: Artech House, 2003.
[8] J. Cha, J. Yi, J. Kim, and B. Kim, "Optimum design of a predistortion RF power amplifier for multicarrier WCDMA applications," *IEEE Trans. Microw. Theory Tech.*, vol. 52, no. 2, pp. 655–663, Feb. 2004.
[9] A. Rabany, L. Nguyen, and D. Rice, "Memory effect reduction for LDMOS bias circuits," *Microw. J.*, vol. 46, no. 2, pp. 124–130, Feb. 2003.
[10] H. Ku, M. D. McKinley, and J. S. Kenney, "Quantifying memory effects in RF power amplifiers," *IEEE Trans. Microw. Theory Tech.*, vol. 50, no. 12, pp. 2843–2849, Dec. 2002.
[11] H. Ku and J. S. Kenney, "Behavioral modeling of nonlinear RF power amplifiers considering memory effects," *IEEE Trans. Microw. Theory Tech.*, vol. 51, no. 12, pp. 2495–2504, Dec. 2003.
[12] C. Eun and E. J. Powers, "A new Volterra predistorter based on the indirect learning architecture," *IEEE Trans. Signal Process.*, vol. 45, no. 1, pp. 223–227, Jan. 1997.
[13] L. Ding, G. T. Zhou, D. R. Morgan, Z. Ma, J. S. Kenney, J. Kim, and C. R. Giardina, "A robust digital baseband predistorter constructed using memory polynomials," *IEEE Trans. Commun.*, vol. 52, no. 1, pp. 159–165, Jan. 2004.
[14] L. Ding, Z. Ma, D. R. Morgan, M. Zierdt, and J. Pastalan, "A least-squares/Newton method for digital predistortion of wideband signals," *IEEE Trans. Commun.*, vol. 54, no. 5, pp. 833–840, May 2006.
[15] T. Liu, S. Boumaiza, and F. M. Ghannouchi, "Deembedding static nonlinearities and accurately identifying and modeling memory effects in wideband RF transmitters," *IEEE Trans. Microw. Theory Tech.*, vol. 53, no. 11, pp. 3578–3587, Nov. 2005.
[16] L. Ding, R. Raich, and G. T. Zhou, "A Hammerstein predistortion linearization design based on the indirect learning architecture," in *Proc. IEEE Int. Acoust., Speech, Signal Process. Conf.*, May 2002, vol. 3, pp. 2689–2692.

[17] D. R. Morgan, Z. Ma, J. Kim, M. G. Zierdt, and J. Pastalan, "A generalized memory polynomial model for digital predistortion of RF power amplifiers," *IEEE Trans. Signal Process.*, vol. 54, no. 10, pp. 3852–3860, Oct. 2006.
[18] T. Liu, S. Boumaiza, and F. M. Ghannouchi, "Augmented Hammerstein predistorter for linearization of broadband wireless transmitters," *IEEE Trans. Microw. Theory Tech.*, vol. 54, no. 4, pp. 1340–1349, Jun. 2006.
[19] S. Chung, J. W. Holloway, and J. L. Dawson, "Open-loop digital predistortion using Cartesian feedback for adaptive RF power amplifier linearization," in *IEEE MTT-S Int. Microw. Symp. Dig.*, Jun. 2007, pp. 1449–1452.
[20] Y. Kim, Y. Yang, S. Kang, and B. Kim, "Linearization of 1.85 GHz amplifier using feedback predistortion loop," in *IEEE MTT-S Int. Microw. Symp. Dig.*, 1998, pp. 1675–1678.
[21] Y. Y. Woo, J. Kim, J. Yi, S. Hong, I. Kim, J. Moon, and B. Kim, "Adaptive digital feedback predistortion technique for linearizing power amplifiers," *IEEE Trans. Microw. Theory Tech.*, vol. 55, no. 5, pp. 932–940, May 2007.
[22] Y. Y. Woo, J. Kim, S. Hong, I. Kim, J. Moon, J. Yi, and B. Kim, "A new adaptive digital predistortion technique employing feedback technique," in *IEEE MTT-S Int. Microw. Symp. Dig.*, Jun. 2007, pp. 1445–1448.
[23] S. Hong, Y. Y. Woo, J. Kim, J. Cha, I. Kim, J. Moon, J. Yi, and B. Kim, "Weighted polynomial digital predistortion for low memory effect Doherty power amplifier," *IEEE Trans. Microw. Theory Tech.*, vol. 55, no. 5, pp. 925–931, May 2007.
[24] S. Haykin, *Adaptive Filter Theory*. Upper Saddle River, NJ: Prentice-Hall, 2001.
[25] "Connected simulation and test solutions using the Advanced Design System," Agilent Technol., Palo Alto, CA, Applicat. Note 1394, 2000.

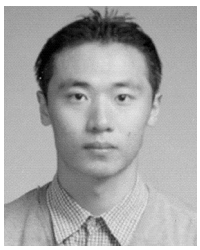

Jangheon Kim (S'07) received the B.S. degree in electronics and information engineering from Chon-buk National University, Chonju, Korea, in 2003, and is currently working toward Ph.D. degree at the Pohang University of Science and Technology (POSTECH), Pohang, Gyeongbuk, Korea.

His current research interests include highly linear and efficient RF PA design, memory-effect compensation techniques, and DPD techniques.

Young Yun Woo received the B.S. degree in electrical and computer engineering from the University of Seoul, Seoul, Korea, in 2006, and is currently working toward the Ph.D. degree at the Pohang University of Science and Technology (POSTECH), Pohang, Gyeongbuk, Korea.

In 2007, he joined the Samsung Electronics Company Ltd., Suwon, Gyeunggi, Korea. His current research interests include RF PA design, LPA system design, and DPD techniques for linearizing high PAs.

Junghwan Moon received the B.S. degree in electrical and computer engineering from the University of Seoul, Seoul, Korea, in 2006, and is currently working toward the Ph.D. degree at the Pohang University of Science and Technology (POSTECH), Pohang, Gyeongbuk, Korea.

His current research interests include highly linear and efficient RF PA design, memory-effect compensation techniques, and DPD techniques.

Bumman Kim (M'78–SM'97–F'07) received the Ph.D. degree in electrical engineering from Carnegie–Mellon University, Pittsburgh, PA, in 1979.

From 1978 to 1981, he was engaged in fiber-optic network component research with GTE Laboratories Inc. In 1981, he joined the Central Research Laboratories, Texas Instruments Incorporated, where he was involved in development of GaAs power field-effect transistors (FETs) and monolithic microwave integrated circuits (MMICs). He has developed a large-signal model of a power FET, dual-gate FETs for gain control, high-power distributed amplifiers, and various millimeter-wave MMICs. In 1989, he joined the Pohang University of Science and Technology (POSTECH), Pohang, Gyungbuk, Korea, where he is a Namko Professor with the Department of Electrical Engineering, and Director of the Microwave Application Research Center, involved in device and circuit technology for RF integrated circuits (RFICs). He was a Visiting Professor of electrical engineering with the California Institute of Technology, Pasadena, in 2001. He has authored over 200 technical papers.

Dr. Kim is a member of the Korean Academy of Science and Technology and the Academy of Engineering of Korea. He was an associate editor for the IEEE TRANSACTIONS ON MICROWAVE THEORY AND TECHNIQUES and a Distinguished Lecturer of the IEEE Microwave Theory and Techniques Society (IEEE MTT-S).